Composites Part B 131 (2017) 91–99

Contents lists available at ScienceDirect

Composites Part B

journal homepage: www.elsevier.com/locate/compositesb

Characterization of recycled thermoplastics-based nanocomposites: Polymer-clay compatibility, blending procedure, processing condition, and clay content effects

Ruey Shan Chen*, Sahrim Ahmad, Sinyee Gan

School of Applied Physics, Faculty of Science and Technology, Universiti Kebangsaan Malaysia, 43600 UKM Bangi, Selangor, Malaysia

ARTICLE INFO

Article history:
Received 6 October 2016
Received in revised form
16 May 2017
Accepted 29 July 2017
Available online 31 July 2017

Keywords:
Polymer-matrix composites (PMCs)
Layered structures
Mechanical properties
Thermal properties

ABSTRACT

Nanocomposites were prepared from recycled polyolefin and clay via melt-blending. The absence/presence of compatibilizer, the blending procedure, and the processing conditions were varied to study their independent effects. First, the compatibilizers ethylene-glycidyl methacrylate (E-GMA) and/or maleic anhydride polyethylene (MAPE) were incorporated with the clay. Second, the initial one-step blending procedure was replaced with a two-step blending procedure in the preparation of the rHDPE/rPET/clay/E-GMA nanocomposite. Third, the extrusion temperature profile and screw rotation speed (30, 60, 90, 120 and 150 rpm) were altered. The overall results from XRD analysis and flexural testing showed that a combination involving the E-GMA compatibilizer, the two-step blending procedure, a high extrusion temperature and a screw rotation speed of 90 rpm was the most effective for obtaining improved clay dispersion and increasing the flexural properties. In the final investigation, various nanoclay contents (1, 3, 5, 7 and 9 wt.%) were introduced. The results showed that the flexural properties, the dispersion of the clay, the thermal stability and the flammability resistance increased with the nanoclay content.

1. Introduction

At present, more than 230 million tonnes of plastics are generated annually, and this value is expected to reach approximately 400 million tonnes in 2020 based on a conservative annual growth rate of approximately 5% [1]. Polyethylene (PE) and polyethylene terephthalate (PET) are used extensively in the field of packaging and account for the majority of plastic waste [2,3]. Post-consumer HDPE from bottles is an interesting recycled material source because it cannot be reused directly and has a high melt viscosity, which causes difficulties in direct transformation through injection moulding [4]. Recently, the technology for recycling post-consumer PET has risen to a very high level. Currently, in addition to the production of fibres and low-cost products, recycled PET (rPET) can also be used in manufacturing high-value engineering materials [5]. One of the easiest approaches to recycling plastic waste is by producing polymer blends and composites [1]. Thermoplastic blends based on HDPE and PET, whether virgin or recycled, have been used as matrices in natural fibre composites [6–9] and nanocomposites [10]. In this study, recycled HDPE (rHDPE) and rPET were selected to create a blend matrix because of their high availability, lower cost but comparable properties to virgin polymer, and environmental friendliness.

The management of plastic wastes can be achieved by simply introducing nanofillers into recycled polymers to produce high-performance and value-added nanocomposites, which are attractive to the polymer and composite industries. Nano-scale additives that serve as fillers promote increased interphase surface areas and high area/volume ratios, resulting in an overall enhancement in performance, including the mechanical properties, dimensional stability, and barrier and gas permeation abilities. Compared to conventional micro-scale fillers, a very small quantity of nanofiller is adequate to obtain outstanding properties without noticeably affecting the density, light transmission properties or cost of the base polymer [1,11]. This beneficial phenomenon is the main reason that these materials are used in a variety of high-performance engineering applications, including aerospace, automotive, infrastructure, construction, and marine applications [12].

Currently, clay is the most commonly used commercial

* Corresponding author.
E-mail address: rueyshanchen@hotmail.com (R.S. Chen).

http://dx.doi.org/10.1016/j.compositesb.2017.07.057
1359-8368/

nanoparticle material, representing almost 70% of the total market value [13]. Because natural clay is inexpensive and environmentally friendly, it has been explored in various applications. Therefore, clay was chosen as the nanofiller in this current study. The interaction between polymer(s) and nanoclays (layered silicates) during the mixing process produces three different types of structures: tactoids (stacking layers), in which the polymer and clay are inherently immiscible; intercalated (well-alternating layered silicates), in which the polymer macromolecule chains reside between the clay layers; and exfoliated, where the stacking layers are destroyed and well-dispersed clay layers reside within the polymeric matrix. Exfoliated silicates with strong adhesion to the polymer are greatly preferred in order to fully exploit the advantages of clay polymer nanocomposites [10,14]. Clay particles are commonly hydrophilic, and thus, their interactions with non-polar (hydrophobic) polymers are unfavourable. Hence, hydrophilic polymers can intercalate within the galleries of Na^+ montmorillonite (MMT) clays, while hydrophobic polymers produce intercalated or exfoliated structures only with organophilic clays, which are formed when hydrated Na^+ ions within the galleries are substituted with the appropriate cationic surfactant, such as alkylammonium, via a cation exchange reaction [14]. However, the dispersion of organically modified clays within nonpolar polymers, such as polypropylene (PP) or polyethylene (PE), remains poorly optimized. Therefore, the introduction of a proper compatibilizer or chemical modification of the polymeric matrix is desirable [15].

Numerous studies on polymer-based nanocomposites have focused on the optimization of the clay content [11,16,17] and the importance of adding a compatibilizer [15,18,19] or chemically modifying the clay [15] to enhance the polymer-clay compatibility, whereas the importance of blending or the compounding method and processing conditions [19] have been studied in very few papers. Additionally, published studies concerning recycled polymers, especially polymer blends, are very limited. Kerboua, Cinausero [20] analysed PET waste/poly(methyl methacrylate) nanocomposites and showed that the incorporation of organo-modified MMT enhanced the compatibility of the blend and the processability and performance of the resultant composites. Hellati, Benachour [21] studied the effects of a styrene–ethylene/butylene–styrene block copolymer grafted with maleic anhydride (SEBS–MAH) compatibilizer on the structure and micromechanical properties of rPET/isotactic PP and rPET/HDPE blends embedded with clay and found that added clay increased the hardness in the presence of a compatibilizer.

Very few researchers have studied the effects of various factors related to compatibility, composition, preparation and mixing on the nanocomposite performance when using recycled thermoplastic blends of rHDPE/rPET as a matrix material. In our previous work, preliminary findings on the tensile strength, impact strength and clay-dispersed structure of nanocomposites made from rHDPE/rPET/clay were obtained [10]. In this current work, the objective was to examine the dispersion of clay layers within the polymers and the flexural properties of the nanocomposites affected by incorporation of a compatibilizer, the blending procedure and the processing conditions during extrusion. The influence of the nanocomposite composition on the relative intercalation, flexural, thermal and flammability properties was investigated by varying the clay content. These studies are crucial to develop useful applications of these materials.

2. Materials and methods

2.1. Raw materials

The thermoplastic polymers, recycled high-density polyethylene (rHDPE), with a melt flow rate of 0.72 g/10 min at 190 °C and a density of 0.923 g/cm^3, and recycled polyethylene terephthalate (rPET), with an intrinsic viscosity of 0.68 dL/g, were obtained from a local plastic recycling plant (Malaysia). Montmorillonite modified with a dimethyl, benzyl, hydrogenated tallow, quaternary ammonium (Cloisite 10A, C10A; CEC = 125 meq/100 g clay and d_{001} = 19.2 Å) was supplied by Southern Clay Products Co., USA. Ethylene-glycidyl methacrylate (E-GMA) and maleic anhydride polyethylene (MAPE) were obtained from BioComposites Extrusion Sdn. Bhd., Malaysia, and had a melt flow rate of 5 g/10 min at 190 °C. Before extrusion, the rPET pellets and C10A were dried at 100 °C for 24 h to remove trapped moisture.

2.2. Preparation of nanocomposites

Melt blending of the composite samples was performed using a laboratory-scale co-rotating twin screw extruder (Thermo Prism TSE 16 PC) with a diameter of 16 mm and a length/diameter ratio of 25. The composition of rHDPE/rPET was maintained at a weight ratio of 75:25 (wt.%). In the first set of experiments, several formulations were selected to examine the influence of the compatibilizer(s) by varying the types of compatibilizer(s) used with 3 wt.% clay and a one-step blending procedure as follows: the formulated raw materials were introduced simultaneously into the hopper,

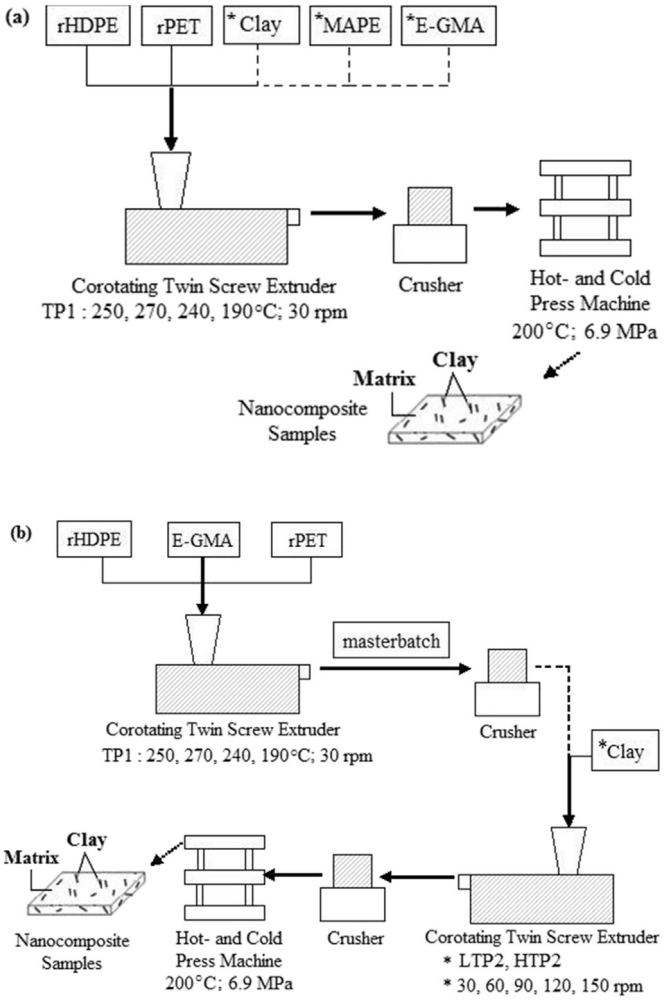

Fig. 1. Scheme for nanocomposite processing by (a) one-step and (b) two-step blending procedure (* Investigated variables).

where the barrel temperature profile (from the feeding to die zone) was set to 190-240-270-250 °C and the screw rotation speed was set to 30 rpm, as shown in Fig. 1(a). The concentration of the E-GMA and MAPE compatibilizers were kept constant at 5% and 3%, respectively, in accordance with the total weight of the composites. To examine the influence of the blending procedure, the nanocomposite with a selected composition (3 wt.% clay and 5% EGMA) was also prepared by a two-step blending procedure (see Fig. 1(b)) as follows: a masterbatch of rHDPE/rPET/E-GMA was first extruded at a barrel temperature profile of 190-240-270-250 °C and a screw rotation speed of 30 rpm. The masterbatch was then mixed with clay following a temperature profile of 170-215-210-195 °C with the same screw rotation speed (30 rpm) during the second extrusion step.

In the second set of experiments, several formulations were selected to study the processing variables by changing the screw rotation speed (30, 60, 90, 120 and 150 rpm) and second extrusion temperature profile (170-215-210-195 °C and 190-240-270-250 °C, denoted LTP2 and HTP2, respectively). It should be noted that the nanocomposite composition (3 wt.% clay, 5% E-GMA) and preparation procedure (two-step blending method) were the same in this case. In the third set of experiments, the influence of the clay concentration (1, 3, 5, 7 to 9 wt.%) was studied, and the type of compatibilizer (E-GMA), preparation procedure (two-step blending method) and processing conditions (LTP and 30 rpm) were the same. Both the second and third sets of nanocomposites were prepared as illustrated in Fig. 1(b).

After extrusion, a hot- and cold-press process using a compression moulding machine (LP50, Labtech Engineering Company, Ltd.) was performed to produce the specimen panels for testing. The upper and lower platen temperature was 200 °C, and a pressure of 6.9 MPa was applied. During hot-pressing, 3 min of preheating, 2 min of venting and 5 min of full hot pressing were applied, followed by 5 min of cold-pressing to cool the panels.

2.3. Characterization techniques

The degree of clay intercalation in the polymer blend/clay nanocomposites was examined by X-ray diffraction (XRD). XRD measurements of powdered clay and the nanocomposite panels were conducted with a D8 Advance diffractometer using CuKα radiation (λ = 0.154056 nm), where the generator power was 40 kV and 30 mA, with scanning (2θ) from 2.3° to 12° at a scanning rate of 2°/min.

Flexural tests were performed at room temperature using a universal testing machine (Testometric M350-10CT) with a crosshead speed of 5 mm/min according to ASTM standard D790-03. The reported mechanical results are the average values of five replicates for each formulation.

Examination of the nanoclay dispersion was carried out using a transmission electron microscope (Philips model STEM CM12) with an acceleration voltage of 100 kV. Prior to TEM observation, the nanocomposite sample was cryo-ultramicrotomed using a Leica UC6 at −80 °C.

Thermogravimetric analysis (TGA) was conducted on approximately 10–15 mg of the samples using a Mettler Toledo TGA/SDTA851[e] at a heating rate of 10 °C/min from 25 °C to 600 °C. Meanwhile, differential scanning calorimetry (DSC) was performed on the 10–15 mg samples, scanning from 25 °C to 300 °C at a heating rate of 10 °C/min, under atmospheric air flow conditions using a Mettler Toledo DSC 882[e].

Burn tests were conducted to determine the relative burning characteristics and flame retardant properties, following ASTM D 5048-90 (Procedure A – test of bar specimens). The burning rates of specimens were computed using the following equation: V = 60 L/t, where V is the burning rate (mm/min), L is the burned length (original length minus the final length) (mm), and t is the burning time (seconds). The reported average results of the burning tests were taken from five replicates for each formulation. The limiting oxygen index (LOI) was determined to measure the minimum oxygen concentration required to support candle-like combustion of the materials. The LOI values of the specimens were determined according to ASTM D 2863 (Procedure A – top surface ignition) using an oxygen index meter. A bomb calorimeter (model 6100 EF) was used to determine the initial enthalpy of the composites. Oxygen at a pressure of 30 atm was purged into the chamber, and the process was monitored using a PARR 6100 EF Jacket Bomb Calorimeter system.

3. Results and discussion

3.1. Clay and compatibilization effects

To attain enhanced mechanical, thermal and flame retardant behaviours of the thermoplastic blend, a homogenous dispersion of nanoparticles whether intercalated or exfoliated in a polymeric matrix, must be fully achieved first. The dispersion level of clay nanofillers within the polymer matrix can be evaluated by the interlayer spacing (d-spacing) of the clay nanofillers and the relative intercalation (RI) of polymer using equations (1) and (2) as follows:

$$n\lambda = 2d \sin\theta \quad (1)$$

$$RI\ (\%) = \frac{d - d_p}{d_p} x100 \quad (2)$$

where n denotes the integer number of the wavelength (n = 1), λ denotes the X-ray wavelength, d denotes the interlayer spacing of the clay in the nanocomposite, θ is half of the diffraction angle, and d_p denotes the interlayer spacing of the clay layers in the pristine clay [22].

Table 1 summarizes the interlayer spacing and relative intercalation of clay in the nanocomposites with different compatibilizers. The pristine clay, i.e., C10A, displayed a characteristic peak at 2θ = 4.56° and had a d-spacing of 19.30 Å. The nanocomposites based on clay showed a peak shift from 4.56° to lower angles in the range of approximately 2.70–2.91°. As reported in our previous work, this phenomenon suggests the intercalation of clay layers within the polymer blend matrix [10]. The nanocomposite compatibilized with E-GMA exhibited a slightly larger d-spacing and a slightly higher RI than its counterparts with other compatibilizers, i.e., MAPE and hybrid MAPE/E-GMA. The diffraction peak of the clay rHDPE/rPET matrix with E-GMA shifted to a lower angle of 2.70°. Both XRD measurements imply an increased compatibility between the polymer blend matrix and the clay with E-GMA, which leads to a higher degree of exfoliation of the nanoclay layers in the nanocomposites [23]. The presence of the more reactive epoxy functionality in GMA may favour the chemical interactions between the polymers and layered silicates; thus, the penetration of polymer chains between the silicate layers was much better in the E-GMA-compatibilized polymer blend/clay nanocomposites.

The reinforcing effects of the nanoclay and the compatibilizing effects of the different compatibilizers on the flexural properties of neat rHDPE/rPET are presented in Fig. 2. As demonstrated by comparing Fig. 2(a) and (b), both the flexural strength and modulus showed similar trends. The use of clay as a nanofiller in the rHDPE/rPET blend without compatibilizer was found to decrease the flexural properties, due to the immiscibility between the rHDPE and rPET components and the incompatibility among rHDPE, rPET

Table 1
Interlayer spacing and relative intercalation of nanocomposites with different compatibilizer.

Nanocomposite Samples	2θ (°)	d-spacing (Å)[a]	Relative Intercalation, RI (%)
Pristine clay	4.56	19.30	–
rHDPE/rPET/Clay	2.91	29.78	54.30
rHDPE/rPET/Clay/MAPE	2.82	30.28	56.84
rHDPE/rPET/Clay/E-GMA	2.70	31.27	62.02
rHDPE/rPET/Clay/MAPE/EGMA	2.72	30.77	59.43

[a] Values obtained from experimental XRD curves.

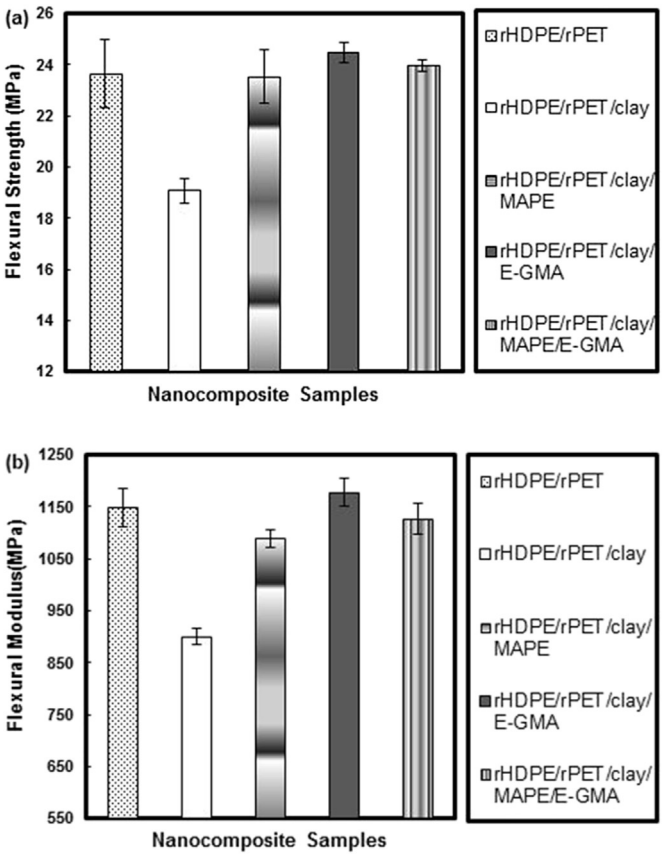

Fig. 2. Flexural properties for nanocomposites with different compatibilizer.

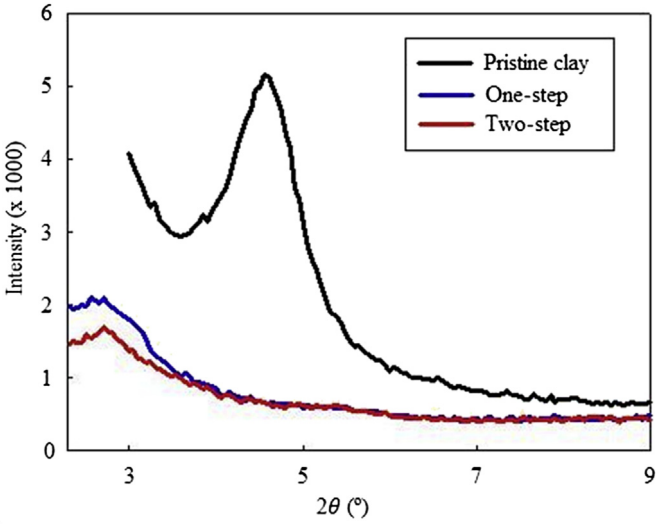

Fig. 3. XRD patterns of the pristine clay and its nanocomposites compounded with different blending procedure.

and clay. According to Chau (2012), the adhesion strength and stiffness of the polymer matrix/nanoclay interface are key factors contributing to the flexural strength of nanocomposites by playing a role in the stress distribution and elastic deformation of the matrix [24]. In the presence of compatibilizer, the flexural strength and modulus of the nanocomposites increased in comparison to the rHDPE/rPET/clay nanocomposites. This process was attributed to enhanced polymer-clay interaction through the incorporation of compatibilizer [18]. The highest flexural strength and modulus values of 24.5 MPa and 1178 MPa, respectively, were achieved by the nanocomposites incorporated with E-GMA. Therefore, as a compatibilizer, E-GMA is the most effective at enhancing the interactions and adhesion between the rHDPE-rPET components and the clay.

3.2. Blending procedure effects

Fig. 3 displays the XRD patterns of the pristine clay and its nanocomposites compounded using different blending procedures, and the XRD measurement data are listed in Table 2. In comparison to one-step blending, the nanocomposites prepared using the two-step blending procedure showed positive properties, such as lower-angle diffraction peak, higher d-spacing and higher RI percentage. As illustrated in Fig. 4, both nanocomposites present intercalated and exfoliated silicate layer systems, as shown by the dark line. The TEM micrograph of the one-step blending procedure indicates that the clay is in the intercalated state, although a certain degree of agglomeration or overlapping of the silicate layers is observed (darker colour in Fig. 4(a) than in the other sample). For the two-step blending procedure, the clay is highly dispersed in the polymer blend matrix and some degree of combined intercalation and exfoliation is observed, as shown in Fig. 4(b). These results are in agreement with the XRD curves. As shown in Table 2, the flexural strength and modulus improved by approximately 31.4% and 7.7%, respectively. These improvements indicate that the two-step blending procedure is appeared as a suitable preparation method for nanoparticles based on polymer blend composites, which leads to better compatibility between the polymer components in the blend and a more effective clay dispersion than the one-step blending procedure.

3.3. Processing condition effects

The effects of the processing conditions on the clay dispersion in the polymer matrix and on the flexural properties are described in Table 3. The extrusion parameters studied in the current work, i.e., the second extrusion temperature profile and screw rotation speed, will be discussed individually.

A comparison of the second extrusion temperature profiles

Table 2
Interlayer spacing, relative intercalation and flexural properties of nanocomposites prepared with different blending procedure.

Blending Procedure	2θ (°)	d-spacing (Å)	Relative Intercalation, RI (%)	Flexural Strength (MPa)	Flexural Modulus (MPa)
One-step	2.70	31.27	62.02	24.5 ± 1.3	1178 ± 17
Two-step	2.65	32.56	68.70	32.2 ± 2.2	1269 ± 23

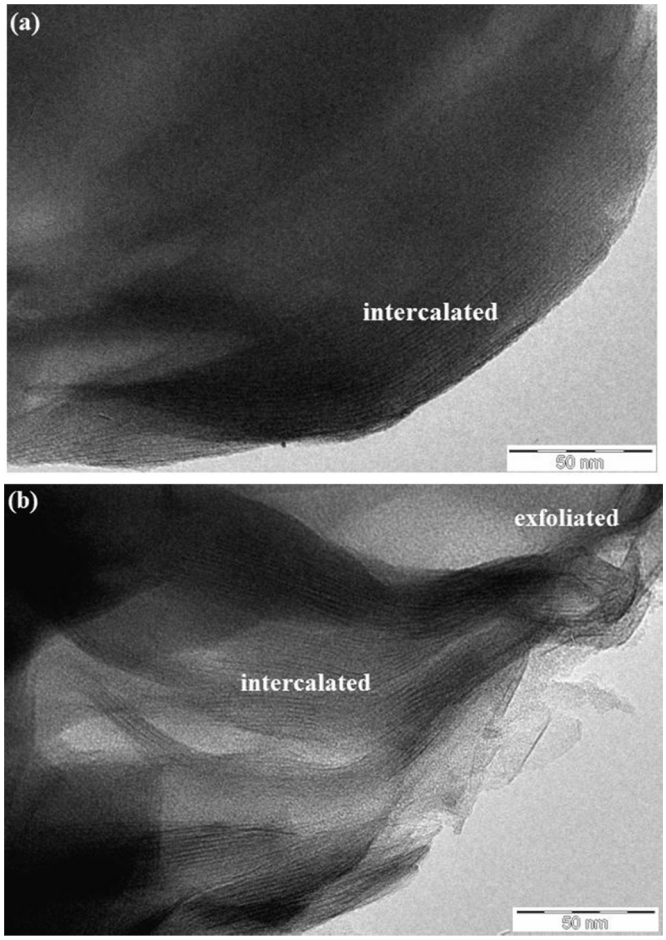

Fig. 4. TEM micrograph of the nanocomposites compounded with (a) one-step (b) two-step blending procedure.

(HTP2 and LTP2) revealed that the nanocomposite extruded at HTP2 exhibited a lower diffraction angle (2θ = 2.61°), a larger distance between the silicate layers (d-spacing = 33.68 Å) and a higher percentage of relative intercalation (74.51%) than that prepared at LTP2. As shown in Fig. 5 (a), the nanocomposite extruded at HTP2 displayed a lower-intensity XRD pattern compared to that extruded at LTP2. These results indicate that a relatively higher extrusion temperature during the introduction of clay into the polymer matrix promoted greater intercalation in the layered silicates. This phenomenon occurred because the higher extrusion temperature accelerated the diffusion of the polymer macromolecule chains into the clay galleries, which enabled the intercalation process to occur before the final degradation of the quaternary ammonium ions in the nanoclay structure [19]. The nanocomposite containing the more intercalated clay exhibited a slightly higher flexural strength and modulus values, which were approximately 33.2 MPa and 1350 MPa, respectively.

As shown in Table 3, the screw rotation speed is another processing condition that affects the dispersion and intercalation of clay. Among the investigated screw rotation speeds, it is clear that the nanocomposite extruded at 90 rpm obtained the highest d-spacing (36.01 Å) and RI percentage (86.58%) and had the lowest XRD peak intensity (Fig. 5(b)), indicating greater intercalation of the polymer chains among the nanoclay layers. Generally, the screw rotation speed is related to the applied shear stress and the residence time of the molten material during the compounding process in the extruder. Increasing the screw speed generates a higher shear stress in the polymer melt, and the increased shear force is sufficient to delaminate the clay nanolayers [25,26]. However, at the same time, the residence time of the molten material decreases with the increasing rotational speed of the extruder screw. According to Zhang, Gao [27], the technical parameters for the production of composites require high shear stress in the molten polymer and suitable residence time in the extruder. In this case, 90 rpm seemed to be the optimum screw rotation speeds and it can be assumed that a higher speed will lead to an inadequate residence times of the melt in the extruder that are inadequate to achieve complete compounding. Incomplete mixing of the composite material leads to poor intercalation of clay layers in the polymer matrix, as shown by the decrease in the d-spacing from 36.01 Å to 32.95 Å (from 90 to 150 rpm). The dispersion and intercalation state of the nanoclay agree with the flexural properties of the nanocomposites, as the highest flexural strength and modulus values were obtained at 90 rpm (34.4 MPa and 1319 MPa, respectively).

3.4. Clay content effects

The effects of the clay content on the interlayer spacing and relative intercalation of nanocomposites are shown in Table 4. As

Table 3
Interlayer spacing, relative intercalation and flexural properties of nanocomposites with different processing condition.

Second Extrusion Temperature Profile	Screw Speed (rpm)	2θ (°)	d-spacing (Å)	Relative Intercalation (%)	Flexural Strength (MPa)	Flexural Modulus (MPa)
HTP2	30	2.61	33.68	74.51	33.2 ± 0.1	1350 ± 39
LTP2	30	2.65	32.56	68.70	32.2 ± 2.2	1269 ± 23
LTP2	60	2.68	32.68	69.33	33.1 ± 1.6	1281 ± 22
LTP2	90	2.63	36.01	86.58	34.4 ± 0.4	1319 ± 16
LTP2	120	2.66	33.04	71.19	32.8 ± 1.9	1278 ± 24
LTP2	150	2.67	32.95	70.73	29.2 ± 2.0	1204 ± 19

Note: HTP2 denotes higher temperature profile during second extrusion; LTP2 denotes lower temperature profile during second extrusion.

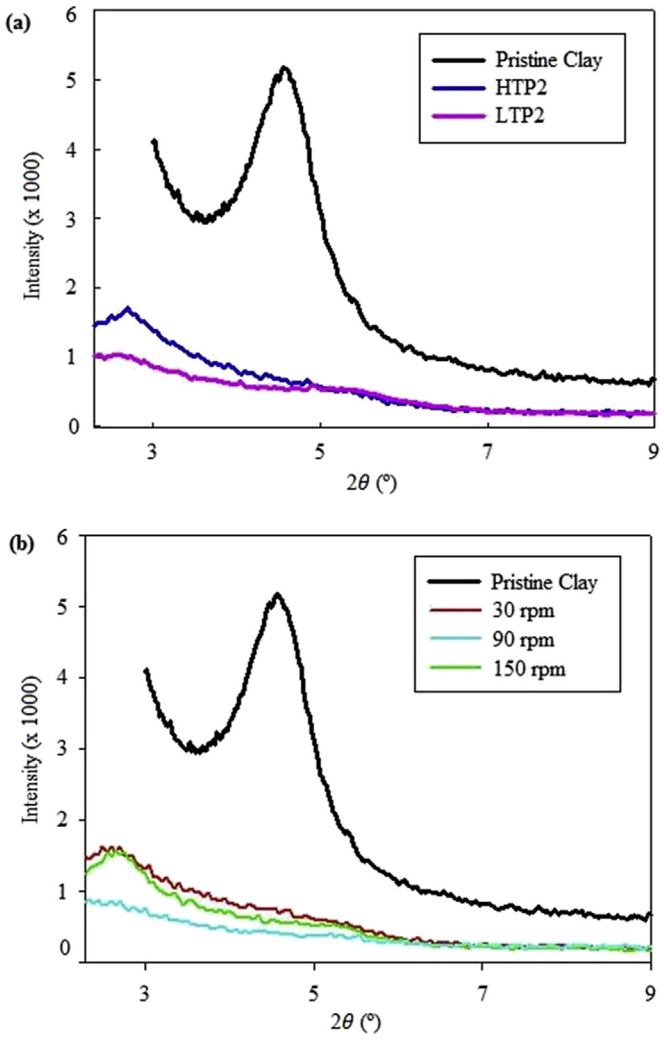

Fig. 5. XRD patterns of the pristine clay and its nanocomposites compounded with different processing condition.

the nanoclay was incorporated into the polymer blend matrix via melt-blending in an extruder, the XRD measurement showed that the characteristic peak of clay shifted to lower angles (2.64–2.77°) and the d-spacing between the clay layers increased (31.64–32.88 Å) compared to pristine clay (2θ = 4.56° and d-spacing of 19.3 Å). When the added clay content was increased from 1 wt.% to 9 wt.%, the characteristic diffraction peak shifted slightly towards higher angles of 2.65°, 2.68°, 2.74° and 2.77°, with a simultaneous decrease in the intensity of the XRD pattern (Fig. 6). On the other hand, the d-spacing between silicate layers, related to the intercalation of the nanoclay, gradually decreased from 32.88 Å to 31.64 Å with increasing nanoclay content. This phenomenon could be ascribed to the dispersion state of clay and the agglomeration of the clay at higher contents.

Table 4
Interlayer spacing and relative intercalation of nanocomposites with different clay content.

Nanocomposite Samples	2θ (°)	d-spacing (Å)	Relative Intercalation (%)
Pristine clay	4.56	19.30	–
1 wt.% clay	2.64	32.88	70.36
3 wt.% clay	2.65	32.56	68.70
5 wt.% clay	2.68	32.30	67.36
7 wt.% clay	2.74	31.96	65.60
9 wt.% clay	2.77	31.64	63.94

As depicted in Fig. 7, both the flexural strength and modulus values showed similar trends, i.e., steep increases at low nanoclay contents (below 3 wt.%) and gentler increases at higher clay contents (above 3 wt.%). The general improvement in the flexural properties is as a result of the good adhesion between the components in the composite. According to Mohan and Kanny [28], an increase in the flexural modulus of a composite containing nanoclay is ascribed to the intercalation or exfoliation of clay nanoparticles in the matrix, which limits the movement of the polymer chains under load. The alignment of clay platelets and polymer chains with respect to the loading direction could contribute to the strengthening effect; however, the rate of the modulus increase gradually decreased at higher clay contents due to the agglomeration of the clay. This observation corresponds to the flexural results in this study.

Fig. 8 displays the (a) thermogravimetric analysis (TGA) and (b) derivative thermogravimetry (DTG) curves of the nanocomposites incorporated with different clay contents. The decomposition temperature (T_d), weight loss and residues above 600 °C for the investigated nanocomposites are given in Table 5. All composites with or without the presence of nanoclay underwent a dramatic weight loss through a one-step degradation process. For the neat polymer blend, the weight loss process began at 365 °C and was almost complete at 508 °C, with 2.74% residues and a maximum decomposition rate at 469 °C. With the addition of nanoclay, there was a significant improvement in the thermal stability with a maximum rate of decomposition at 472–483 °C and residues of approximately 4.43–9.41%. As the clay content increased from 1 wt.% to 9 wt.%, T_d shifted to higher temperatures, and the amount of residues remaining after combustion at 600 °C continued to increase. This can be attributed to the nature of the intercalated silicate layers which delayed the formation of volatile products at the scission temperature of the carbon-carbon polymer [17,29].

Fig. 9 shows the DSC heating curves of the nanocomposites with different clay contents. Table 6 lists the melting temperature (T_m) and crystallinity (χ_c) of all the investigated nanocomposites. For the composites containing nanoclay, the T_m values of the rHDPE and rPET components were higher than those of the neat polymer blend without clay. This observation suggests that the thermal stability of

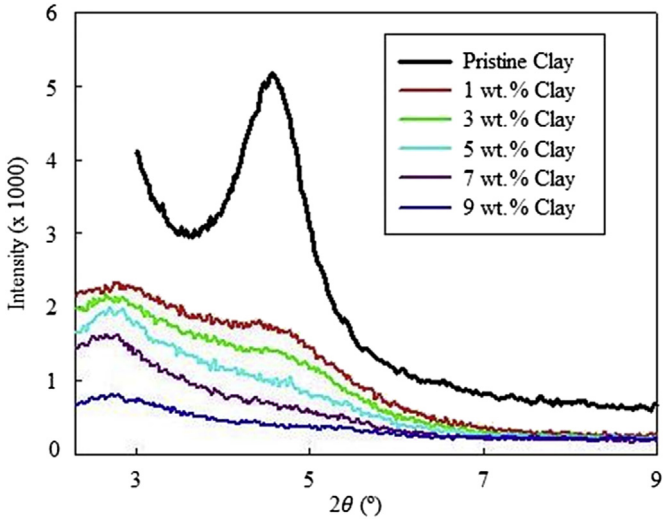

Fig. 6. XRD patterns of the pristine clay and its nanocomposites different clay content.

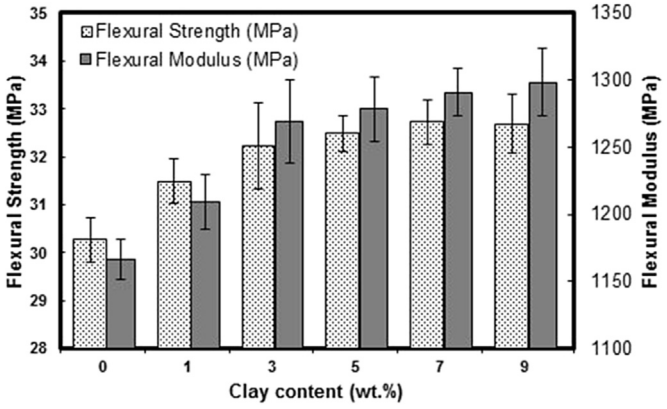

Fig. 7. Flexural properties for nanocomposites with different clay content.

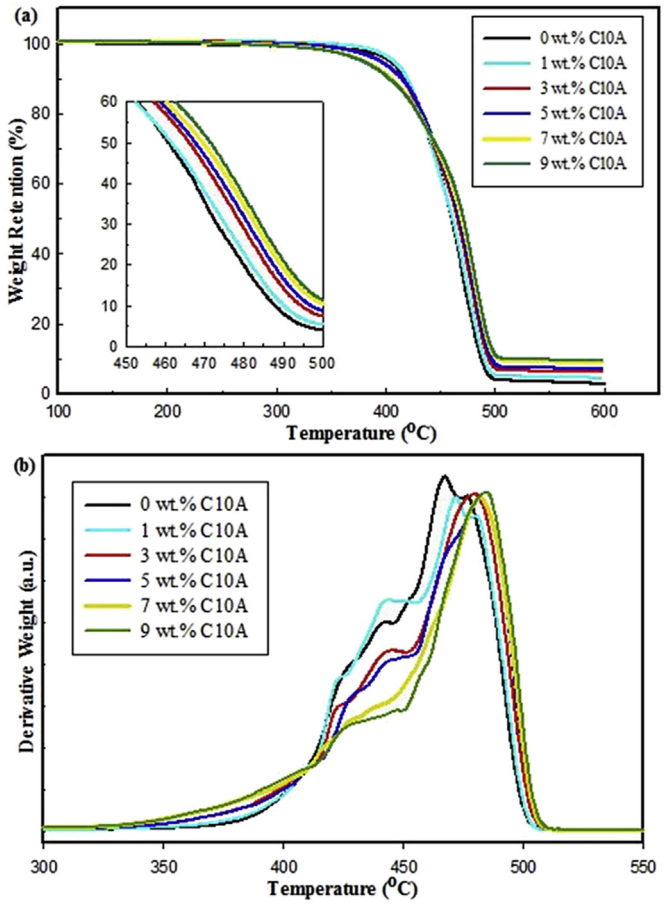

Fig. 8. (a) Thermogravimetric analysis (TGA) and (b) Derivative thermogravimetry (DTG) curves for nanocomposites with different clay content.

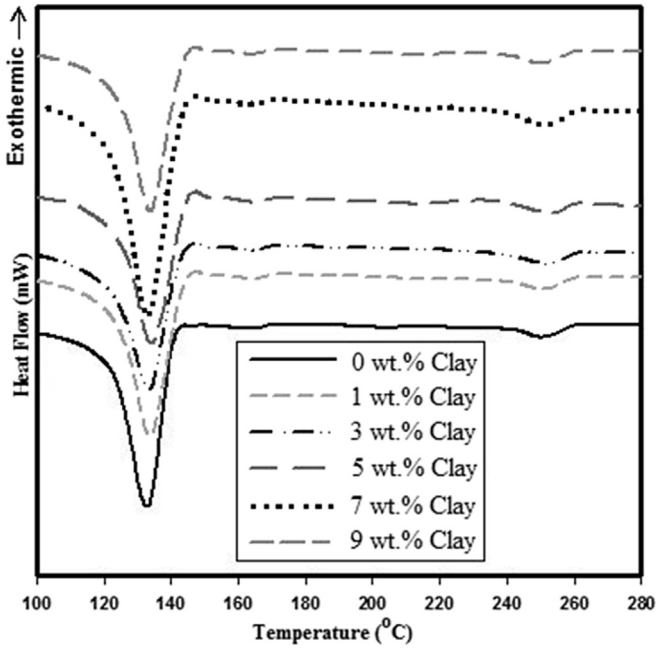

Fig. 9. DSC heating curves for nanocomposites with different clay content.

Table 6
Melting temperature (T_m) and crystallinity level (χ_c) for nanocomposites with different clay content.

Clay Content (wt.%)	HDPE Component		PET Component	
	T_m (°C)	χ_c (%)	T_m (°C)	χ_c (%)
0	133.6	54.9	251.2	20.6
1	134.9	49.5	251.7	18.2
3	135.2	53.0	254.5	15.1
5	135.7	47.2	254.2	13.5
7	135.0	41.3	252.6	11.0
9	135.0	42.8	252.1	10.1

the nanocomposite was improved by the addition of nanoclay. The highest melting temperatures of the rHDPE and rPET components (135.7 °C and 254.5 °C, respectively) were observed in the nanocomposites with 3 wt.% clay. When over 5 wt.% clay was incorporated, the T_m of the polymers decreased significantly. According to a study by Cui and Woo [30] on PE/clay prepared via in situ polymerization with a vanadium-based intercalation catalyst, T_m shifts to higher values at higher clay contents because the clay layers have good barrier action and the strong PE-clay interaction can limit the movement of polymer chains.

As seen in Table 6, the nanocomposites containing 1–9 wt.% clay exhibited lower crystallinity (χ_c) values for both the HDPE and PET components compared to the neat polymer blend. This result is

Table 5
Decomposition temperature, weight loss and residues for nanocomposites with different clay content.

Clay Content (wt.%)	Decomposition Temperature, T_d (°C)	Weight Loss at T_d (%)	Residues after 600 °C (%)
0	469	97.54	2.74
1	472	95.80	4.43
3	479	93.99	6.18
5	482	93.17	7.07
7	482	91.24	9.02
9	483	90.74	9.41

Table 7
Flammability behavior, burning rate and limiting oxygen indices (LOI) for nanocomposites with different clay content.

Clay Content (wt.%)	Flame Characteristics	Charred Ash	Burning Rate (mm/min)	LOI (%)
0	Pronounced dripping, black smoke	Negligible	42.4 ± 1.0	12.6
1	Drips, black smoke	Yes	36.9 ± 1.0	13.1
3	Drips, black smoke	Yes	33.5 ± 0.5	13.4
5	Drips, black smoke	Yes	33.0 ± 0.2	14.2
7	Drips, black smoke	Yes	32.6 ± 0.4	13.2
9	Drips, black smoke	Yes	31.9 ± 0.3	12.9

supported by the works of Lei, Wu [31], who produced rHDPE/clay, and Entezem, Khonakdar [16], who studied PP/PET/clay. Therefore, clay can serve as a nucleating agent for the crystallization of polymer chains; however, clay can also suppress the crystallization by inhibiting the mobility of polymer chains via the formation of a network-like structure [16,32]. In this study, the latter effect can be considered a possible cause of the reduced crystallinity.

The flammability behaviours and burning rates of the nanocomposites with different clay contents are listed in Table 7. Notably, the combustion behaviours of the blend (without clay) and the nanocomposites (with clay) were similar: the samples burned with dripping and released black smoke. The burning rate of the nanocomposites decreased with an increase in the nanoclay content by approximately 13–25% in comparison to the neat polymer blend (42.4 mm/min). Therefore, the flammability resistance of the nanocomposites was enhanced. The proposed mechanism for the clay nanocomposite involves the formation of ash and alumina-silica, which act as a potential barrier for mass and energy transport by delaying the heat transfer and diffusion of oxygen during combustion. A ceramic-like layer was produced on the surface of the composite material, and the efficiency is dependent upon the homogeneity of the layer [33].

As shown in Table 7, the neat polymer blend had the lowest LOI value of approximately 12.6%. This value improved slightly after the incorporation of clay to the neat polymer blend and the highest LOI value was obtained by the nanocomposite containing 5 wt.% clay. Deka and Maji reported that the presence of nanoclay slowed flame propagation in the composite due to silicate char formation on its surface. Compared to the 5 wt.% clay nanocomposite, the lower LOI values of the 7–9 wt.% clay nanocomposites were attributed to poor dispersion and clay agglomeration in the composites [29].

As shown in Fig. 10, the highest combustion enthalpy was found for the control sample (neat polymer blend), i.e., 41,807.52 J/g. This enthalpy decreased with the increase in the clay content in the composites. This phenomenon is ascribed to the fact that a lower amount of energy is required to break the bonds in the nanocomposites. The presence of clay played a crucial role in the combustion process by releasing free radicals that bonded with the applied oxygen, which subsequently reduced the hydrogen atoms and broke the organic chains [34]. Hence, the burning rate of the nanocomposite materials was reduced.

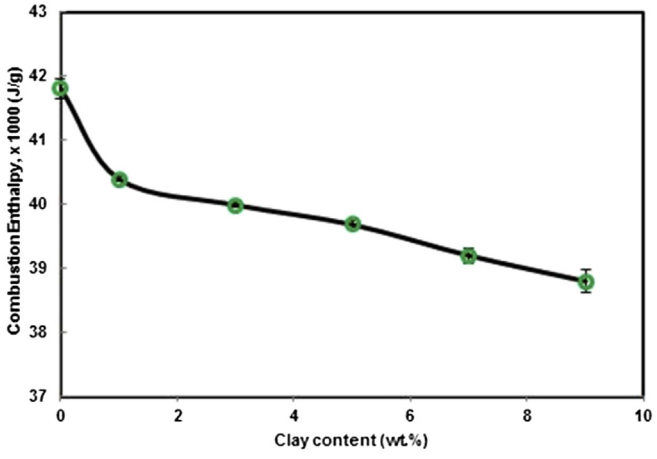

Fig. 10. Heat released (combustion enthalpy) for nanocomposites with different clay content.

4. Conclusions

The introduction of nanoclay incorporated with E-GMA compatibilizer into a rHDPE/rPET blend exhibited the highest polymer-clay miscibility and compatibility, as well as the best flexural properties. Nanocomposite preparation via the two-step blending procedure appeared to be a better approach than one-step blending due to the enhanced clay dispersion obtained in the former method. A higher second extrusion temperature and a screw rotation speed of 90 rpm produced the greatest enhancement in the flexural properties and the relative intercalation of clay layers. As the nanoclay content increased from 1 wt.% to 9 wt.%, the flexural strength and modulus, thermal stability and flame retardancy increased gradually.

Acknowledgements

The authors gratefully acknowledge The National University of Malaysia for the financial support of research grants (DIP-2016-023 and FRGS/1/2014/SG06/UKM/01/2), and Bio Composites Extrusion Sdn Bhd for the donation of materials.

References

[1] Zare Y. Recent progress on preparation and properties of nanocomposites from recycled polymers: a review. Waste Manage 2013;33(3):598–604.
[2] Chen RS, Ab Ghani MH, Ahmad S, Salleh MN, Tarawneh Ma A. Rice husk flour biocomposites based on recycled high-density polyethylene/polyethylene terephthalate blend: effect of high filler loading on physical, mechanical and thermal properties. J Compos Mater 2015;49(10):1241–53.
[3] Chen RS, Ab Ghani MH, Salleh MN, Ahmad S, Tarawneh Ma A. Mechanical, water absorption, and morphology of recycled polymer blend rice husk flour biocomposites. J Appl Polym Sci 2015:132.
[4] Sánchez-Soto M, Rossa A, Sánchez AJ, Gámez-Pérez J. Blends of HDPE wastes: study of the properties. Waste Manage 2008;28:2565–73.
[5] Guntis J, Rita B, Janis Z, Remo Merijs M, Tatjana I, Valdis K, et al. Manufacturing, structure and properties of recycled polyethylene terephthalate/liquid crystal polymer/montmorillonite clay nanocomposites. IOP Conf Ser Mater Sci Eng 2013;49(1):012034.
[6] Chen RS, Ahmad S, Gan S, Salleh MN, Ab Ghani MH, Tarawneh MaA. Effect of polymer blend matrix compatibility and fibre reinforcement content on thermal stability and flammability of ecocomposites made from waste materials. Thermochim Acta 2016;640:52–61.
[7] Chen RS, Ahmad S, Gan S. Characterization of rice husk-incorporated recycled thermoplastic blend composites 2016;11(4). 2016.
[8] Lei Y, Wu Q. High density polyethylene and poly(ethylene terephthalate) *in situ* sub-micro-fibril blends as a matrix for wood plastic composites. Compos Part A 2012;43:73–8.
[9] Lei Y, Wu Q. Wood plastic composites based on microfibrillar blends of high density polyethylene/poly(ethylene terephthalate). Bioresour Technol 2010;101(10):3665–71.

[10] Chen RS, Ahmad S, Gan S, Ab Ghani MH, Salleh MN. Effects of compatibilizer, compounding method, extrusion parameters, and nanofiller loading in clay-reinforced recycled Hdpe/Pet nanocomposites. J Appl Polym Sci 2015;132(29):9180–8.
[11] David R, Tambe SP, Singh SK, Raja VS, Kumar D. Thermally sprayable grafted LDPE/nanoclay composite coating for corrosion protection. Surf Coat Technol 2011;205:5470–7.
[12] Biswal M, Mohanty S, Nayak SK. Influence of organically modified nanoclay on the performance of pineapple leaf fiber-reinforced polypropylene nanocomposites. J Appl Polym Sci 2009;114(6):4091–103.
[13] Silvestre C, Duraccio D, Cimmino S. Food packaging based on polymer nanomaterials. Prog Polym Sci 2011;36:1766–82.
[14] Chrissopoulou K, Anastasiadis SH. Polyolefin/layered silicate nanocomposites with functional compatibilizers. Eur Polym J 2011;47(4):600–13.
[15] Pettarin V, Frontini PM, Pita VJRR, Dias ML, Diaz FV. Polyethylene/(organo-montmorillonite) composites modified with ethylene/methacrylic acid copolymer: morphology and mechanical properties. Compos Part A 2008;39:1822–8.
[16] Entezem M, Khonakdar HA, Yousefi AA, Jafari SH, Wagenknecht U, Heinrich G. On nanoclay localization in polypropylene/poly(ethylene terephthalate) blends: correlation with thermal and mechanical properties. Mater Des 2013;45:110–7.
[17] Biswal M, Mohanty S, Nayak SK. Thermal stability and flammability of banana-fiber-reinforced polypropylene nanocomposites. J Appl Polym Sci 2012;125(S2):E432–43.
[18] Supri AG, Salmah H, Hazwan K. Low density polyethylene-nanoclay composites: the effect of poly(acrylic acid) on mechanical properties, XRD, morphology properties and water absorption. Malays Polym J 2008;3(2):39–53.
[19] Lertwimolnun W, Vergnes B. Influence of compatibilizer and processing conditions on the dispersion of nanoclay in a polypropylene matrix. Polymer 2005;46(10):3462–71.
[20] Kerboua N, Cinausero N, Sadoun T, Lopez-Cuesta JM. Effect of organoclay in an immisicible poly(ethylene terephthalate) waste/poly(methyl methacrylate) blend. J Appl Polym Sci 2010;117:129–37.
[21] Hellati A, Benachour D, Cagiao M, Boufassa S, Baltá Calleja F. Role of a compatibilizer in the structure and micromechanical properties of recycled poly (ethylene terephthalate)/polyolefin blends with clay. J Appl Polym Sci 2010;118(3):1278–87.
[22] Faruk O, Matuana LM. Nanoclay reinforced HDPE as a matrix for wood-plastic composites. Compos Sci Technol 2008;68(9):2073–7.
[23] Tarapow JA, Bernai CR, Alvarez VA. Mechanical properties of polypropylene/clay nanocomposites: effect of clay content, polymer/clay compatibility, and processing conditions. J Appl Polym Sci 2009;111:768–78.
[24] Chau DV. A study on water absorption and its effects on strength of nano organoclay-epoxy composites. J Appl Sci 2012;12:1939–45.
[25] Kord B, Kiakojouri SMH. Effect of nanoclay dispersion on physical and mechanical properties of wood flour/polypropylene/glass fiber hybrid composites. BioResources 2011;6(2):1741–51.
[26] Mohan TP, Kanny K. Effects of synthetic and processing methods on dispersion characteristics of nanoclay in polypropylene polymer matrix composites. Mater Sci Appl 2011;2:785–800.
[27] Zhang Z-X, Gao C, Xin ZX, Kim JK. Effects of extruder parameters and silica on physico-mechanical and foaming properties of PP/wood-fiber composites. Compos Part B Eng 2012;43:2047–57.
[28] Mohan TP, Kanny K. Water barrier properties of nanoclay filled sisal fibre reinforced epoxy composites. Compos Part A 2011;42:385–93.
[29] Deka BK, Maji TK. Study on the properties of nanocomposite based on high density polyethylene, polypropylene, polyvinyl chloride and wood. Compos Part A Appl S 2011;42(6):686–93.
[30] Cui L, Woo S. Preparation and characterization of polyethylene (PE)/clay nanocomposites by in situ polymerization with vanadium-based intercalation catalyst. Polym Bull 2008;61(4):453–60.
[31] Lei Y, Wu Q, Clemons CM, Yao F, Xu Y. Influence of nanoclay on properties of HDPE/wood composites. J Appl Polym Sci 2007;106(6):3958–66.
[32] Bizarria MTM, ALFdM Giraldi, Carvalho CMd, Velasco JI, Ávila MAD, Mei LHI. Morphology and thermomechanical properties of recycled PET-organoclay nanocomposites. J Appl Polym Sci 2007;104:1839–44.
[33] Samyn F, Bourbigot S, Jama C, Bellayer S. Fire retardancy of polymer clay nanocomposites: is there an influence of the nanomorphology? Polym Degrad Stab 2008;93(11):2019–24.
[34] Badri KH, Redwan AM. Effect of phosphite loading on the mechanical and fire properties of palm-based polyurethane. Sains Malays 2010;39(5):769–74.